Electronic Supplementary Information

Perpendicularly aligned nanodomains on versatile substrates *via* rapid thermal annealing assisted by liquid crystalline ordering in block copolymer films

Ting Qu,[a] Song Guan,[a] Xiaoxiong Zheng,[a] and Aihua Chen*[a]

[a]School of Materials Science and Engineering, Beihang University, Beijing 100191, P. R. China

*E-mail: chenaihua@buaa.edu.cn

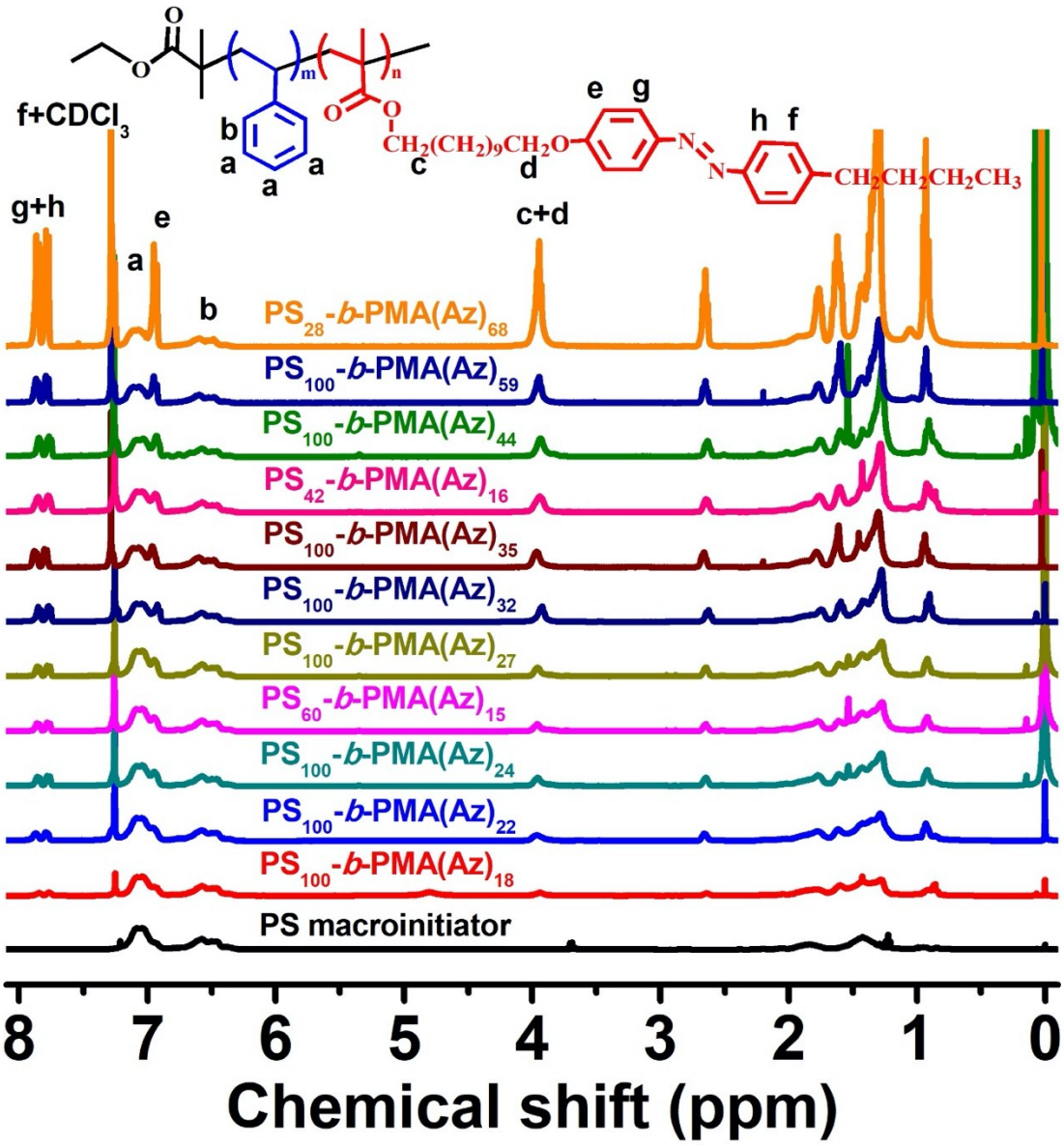

Fig. S1 ^{1}H NMR spectra of PS macroinitiators and PS-*b*-PMA(Az) BCPs.

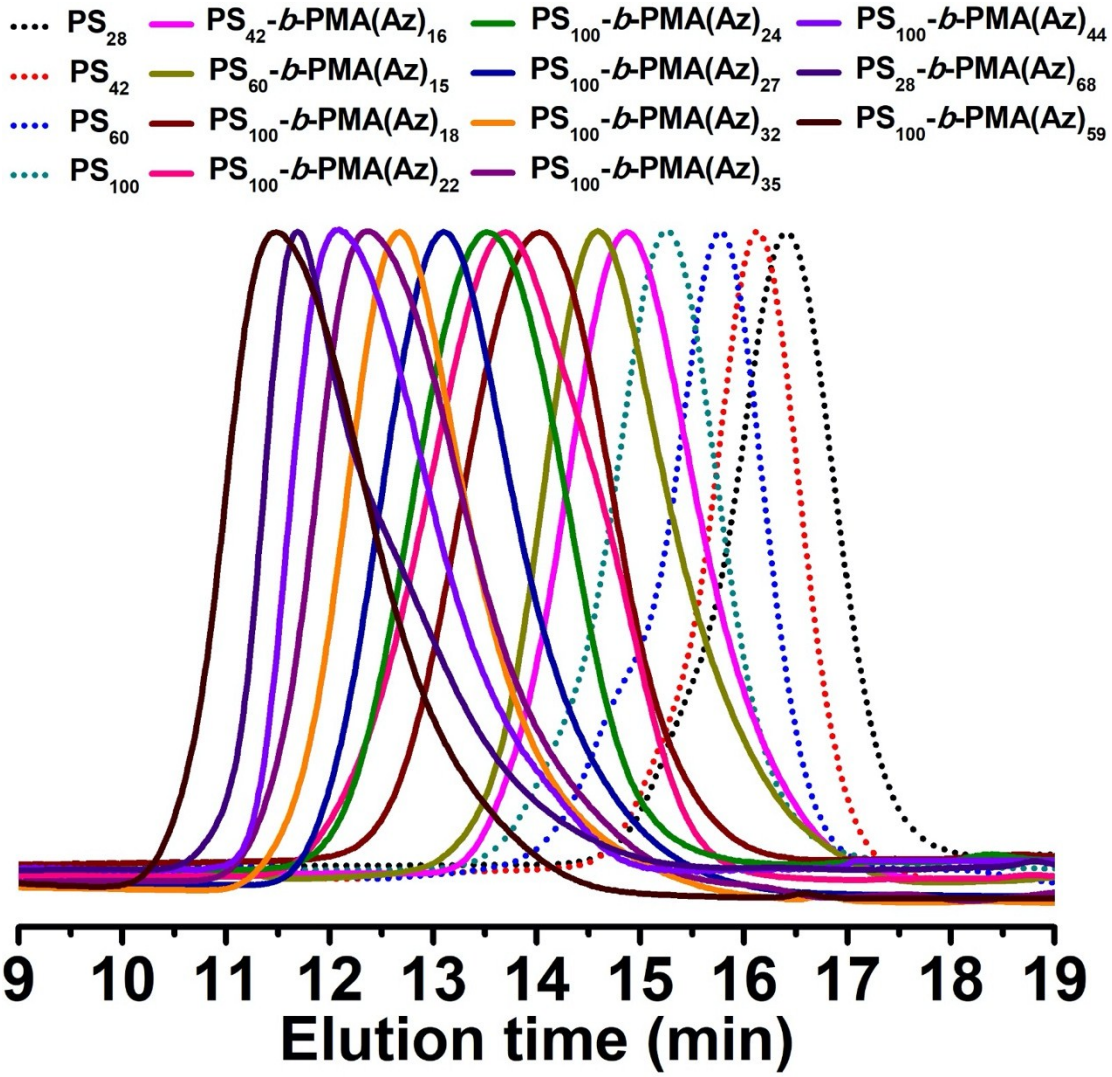

Fig. S2 GPC curves of the PS macroinitiators and PS-*b*-PMA(Az) BCPs with THF as eluent.

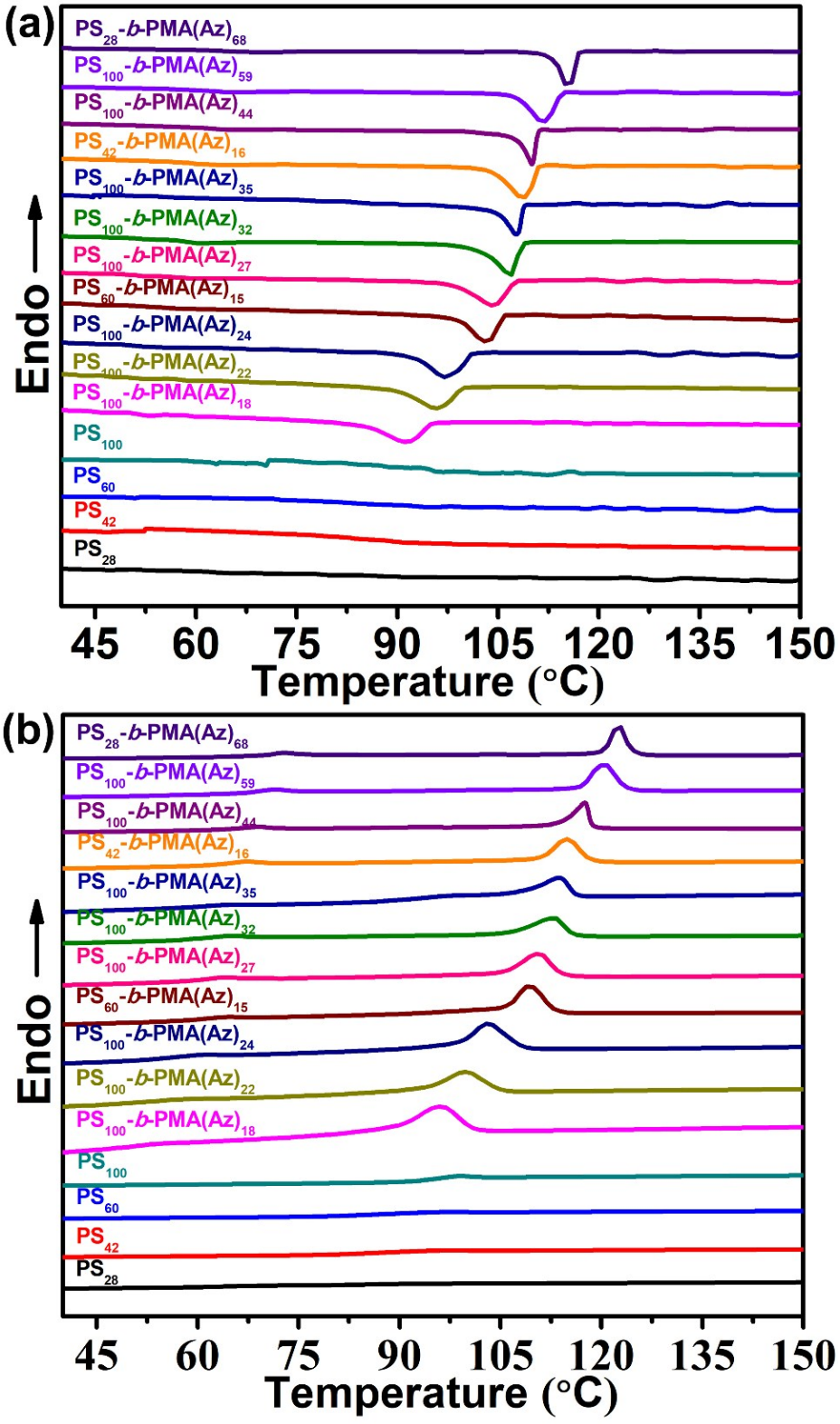

Fig. S3 DSC curves of polymers on the first cooling (a) and second heating (b) processes with a heating/cooling rate of ± 10 °C min^{-1}.

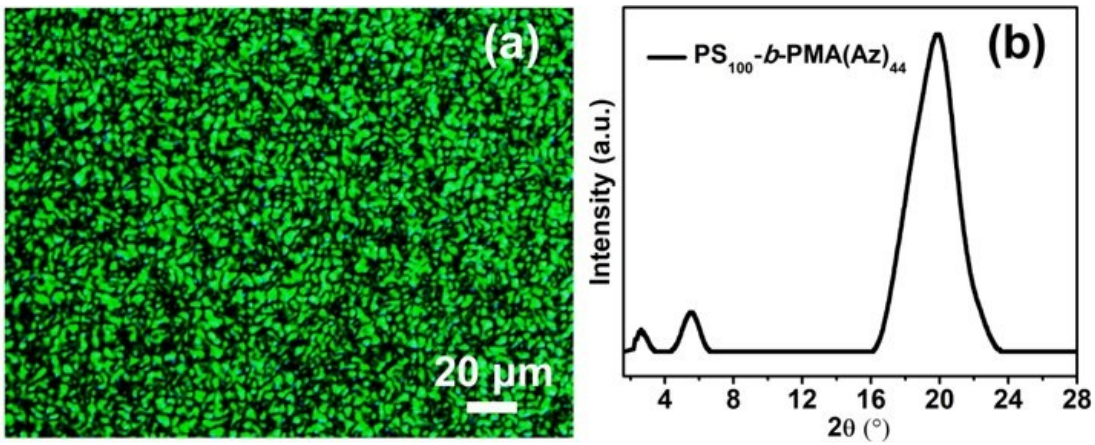

Fig. S4 POM image (a) and WAXD profile (b) of the PS_{100}-*b*-$PMA(Az)_{44}$ samples.

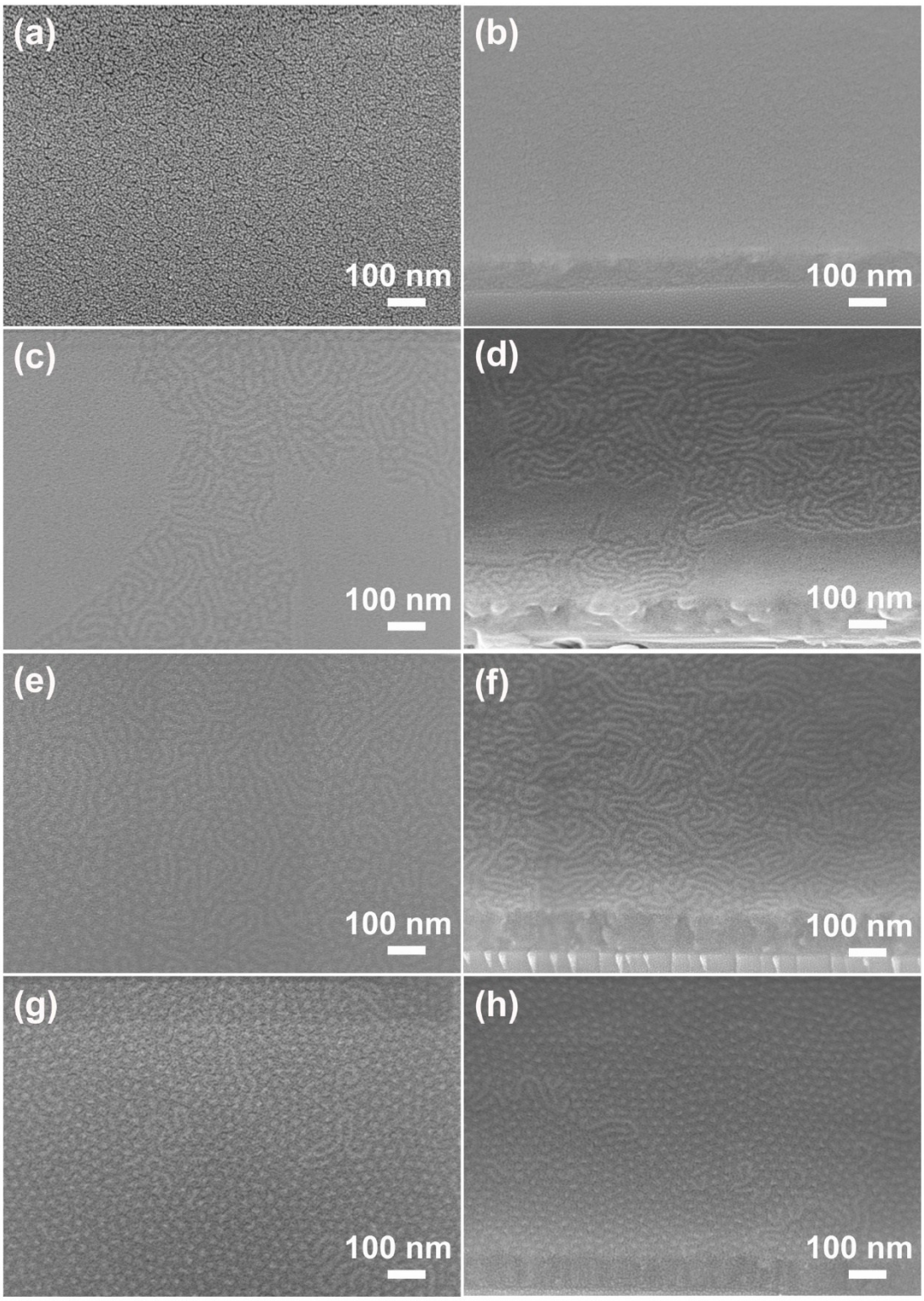

Fig. S5 SEM top (a, c, e, g) and cross-sectional (b, d, f, h) images of PS_{100}-*b*-$PMA(Az)_{44}$ thin films after thermal annealing at 140 °C for different times before RIE: (a, b) 0 min, (c, d) 1 min, (e, f) 3 min and (g, h) 5 min.

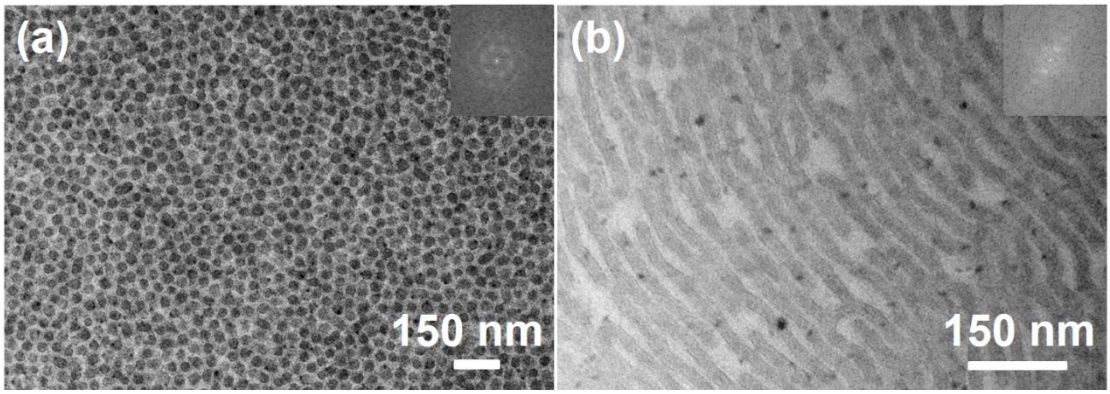

Fig. S6 TEM images (inset: FFT images) of cylindrical PS_{100}-*b*-$PMA(Az)_{44}$ (a) and lamellar PS_{100}-*b*-$PMA(Az)_{22}$ (b) thin films after thermal annealing at 140 °C for 5 min.

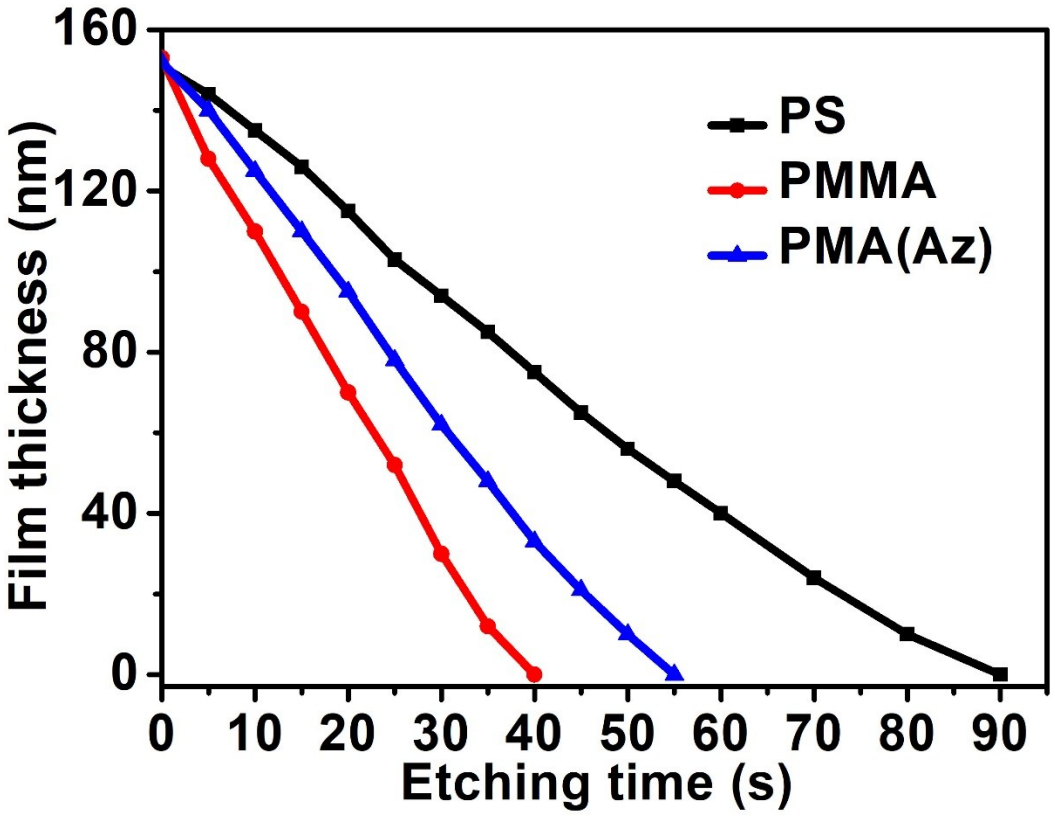

Fig. S7 The etching rate of PS, PMMA and PMA(Az) polymer films at the same RIE conditions: O_2/Ar (40/10) sccm/50 W/75 mTorr.

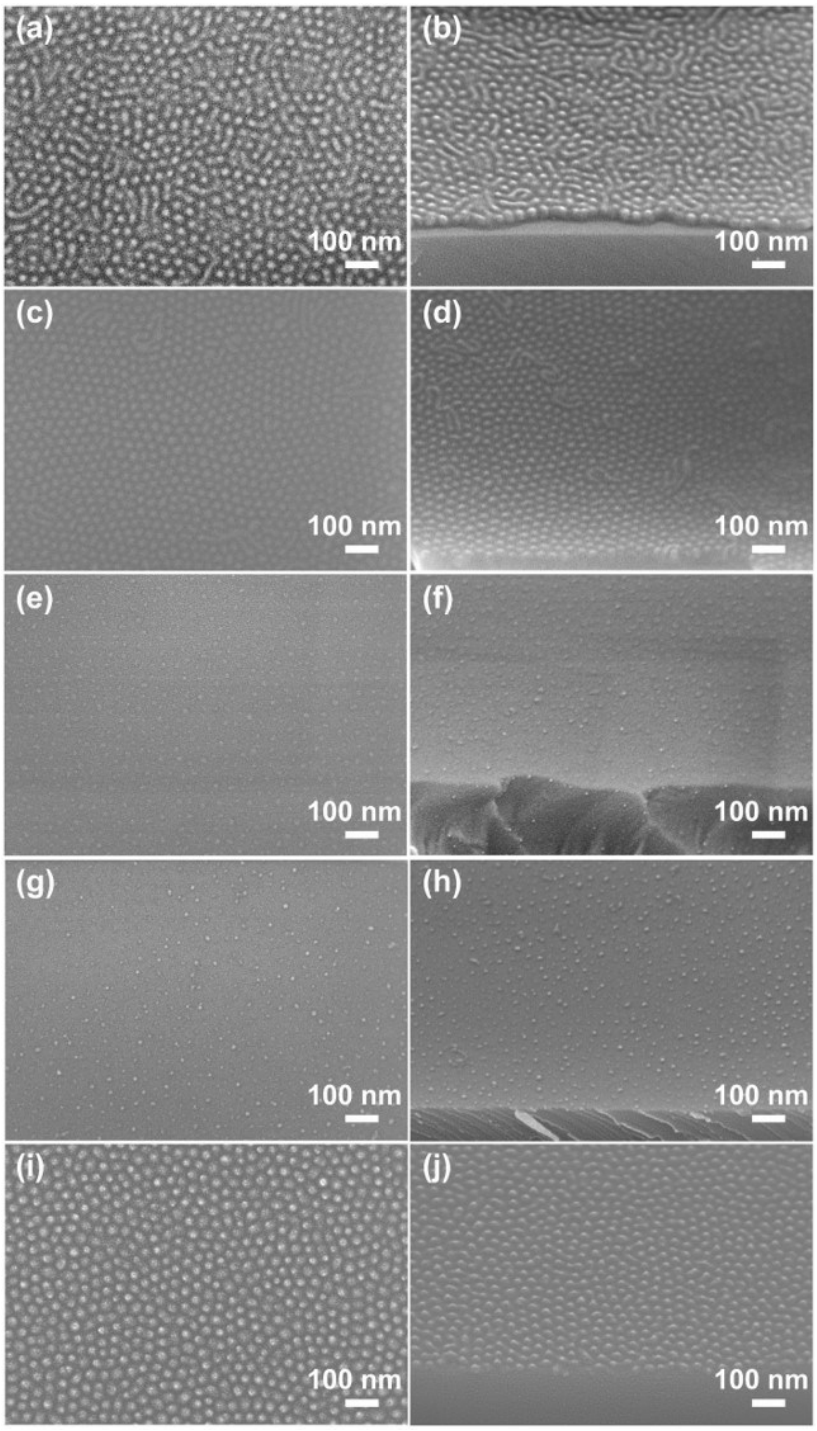

Fig. S8 SEM images of PS_{100}-*b*-$PMA(Az)_{44}$ self-assembled cylindrical films after different RIE conditions: (a, b) O_2/50 sccm/50 W/75 mTorr/30 s, (c, d) O_2/Ar (15/3) sccm/50 W/75 mTorr/30 s, (e, f) O_2/Ar (40/10) sccm/100 W/75 mTorr/30 s, (g, h) O_2/Ar (40/10) sccm/50 W/75 mTorr/60 s, (i, j) O_2/Ar (40/10) sccm/50 W/75 mTorr/30 s.

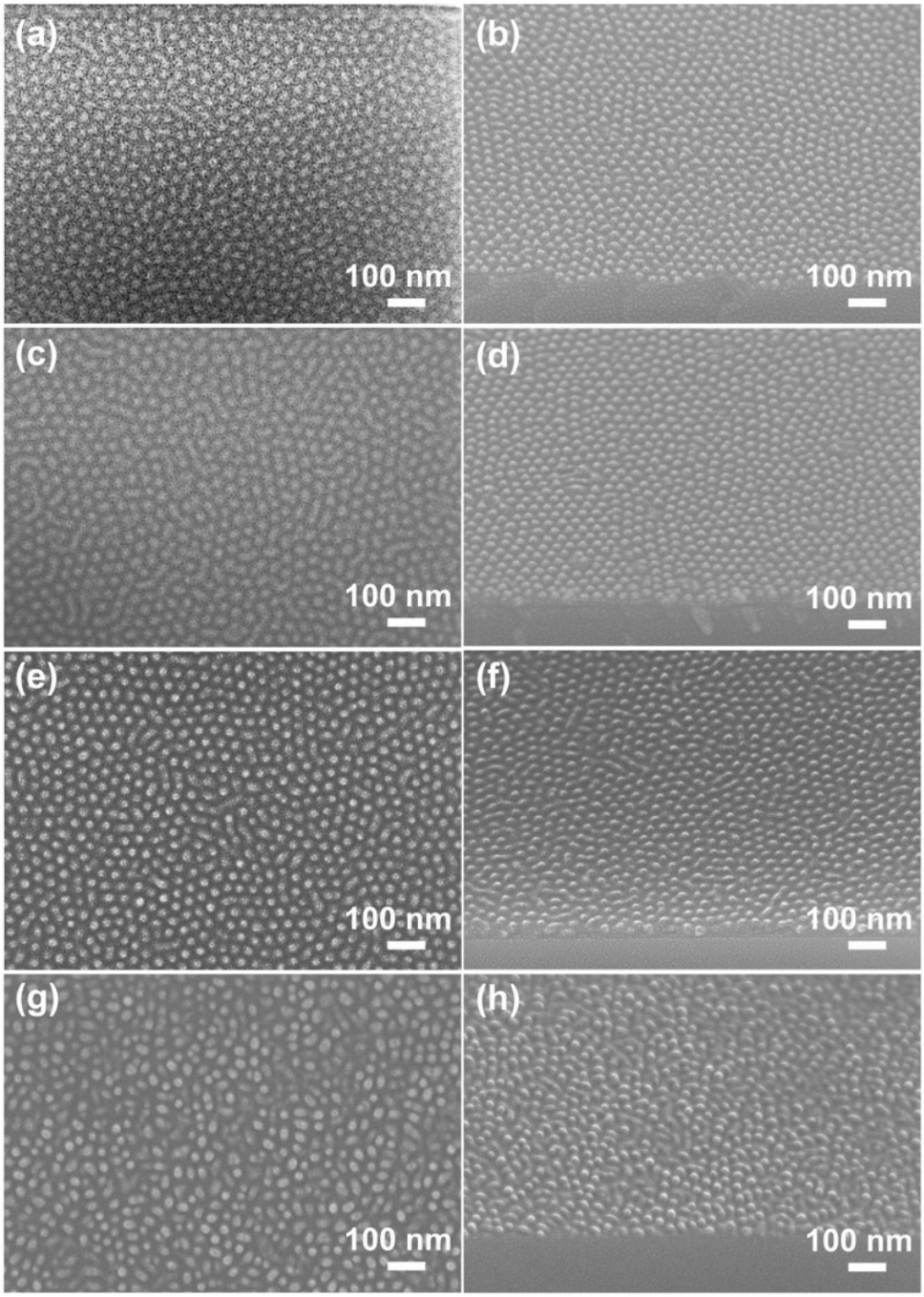

Fig. S9 SEM top (a, c, e, g) and cross-sectional (b, d, f, h) images of PS_m-*b*-$PMA(Az)_n$ self-assembled cylindrical films with different diameters after RIE: O_2/Ar (40/10) sccm/50 W/75 mTorr/30 s. (a, b) PS_{100}-*b*-$PMA(Az)_{59}$, (c, d) PS_{100}-*b*-$PMA(Az)_{35}$, (e, f) PS_{100}-*b*-$PMA(Az)_{32}$, (g, h) PS_{100}-*b*-$PMA(Az)_{27}$, respectively.

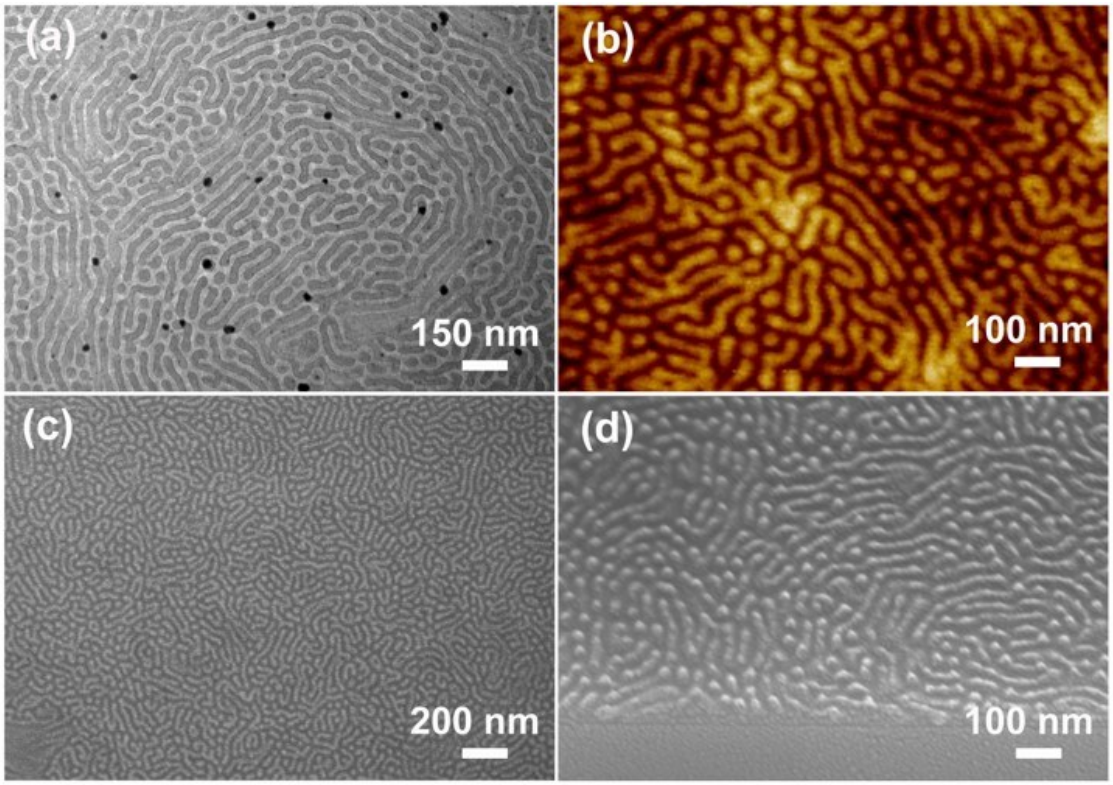

Fig. S10 TEM (a) and AFM (b) images of PS_{100}-*b*-$PMA(Az)_{24}$ self-assembled thin films. SEM top (c) and cross-sectional (d) images of above films after RIE: O_2/Ar (40/10) sccm/50 W/75 mTorr/30 s.

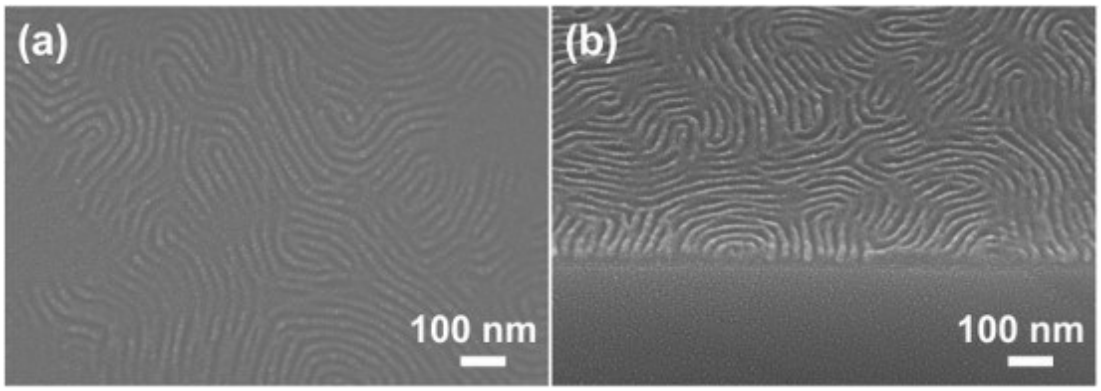

Fig. S11 SEM top (a) and cross-sectional (b) images of PS_{100}-*b*-$PMA(Az)_{18}$ self-assembled lamellar films after RIE: O_2/Ar (40/10) sccm/50 W/75 mTorr/30 s.

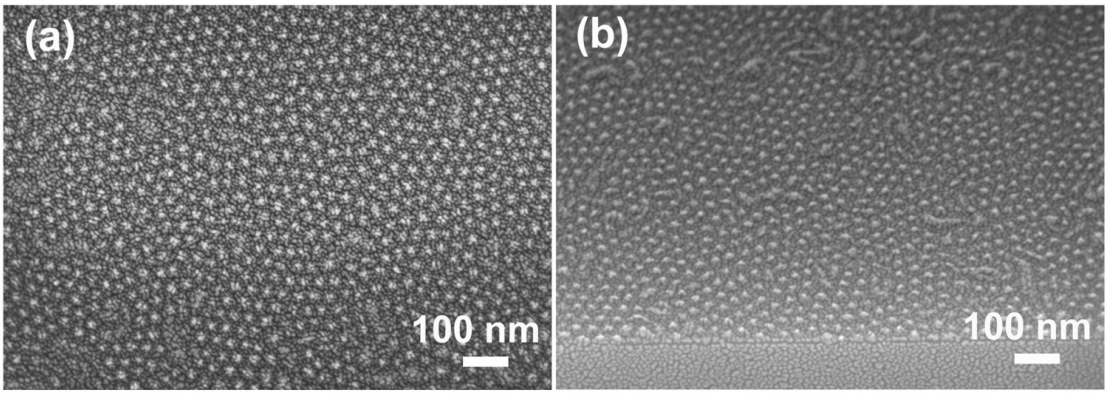

Fig. S12 SEM top (a) and cross-sectional (b) images of PS_{42}-*b*-$PMA(Az)_{16}$ films after RIE: O_2/Ar (40/10) sccm/50 W/75 mTorr/30 s.

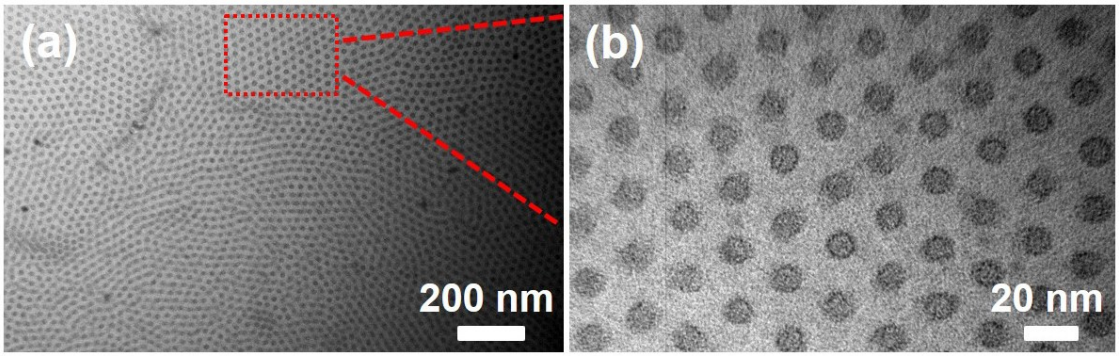

Fig. S13 (a) TEM image of cylindrical PS_{28}-*b*-$PMA(Az)_{68}$ thin film. (b) The magnification of the boxed area inserts in (a).

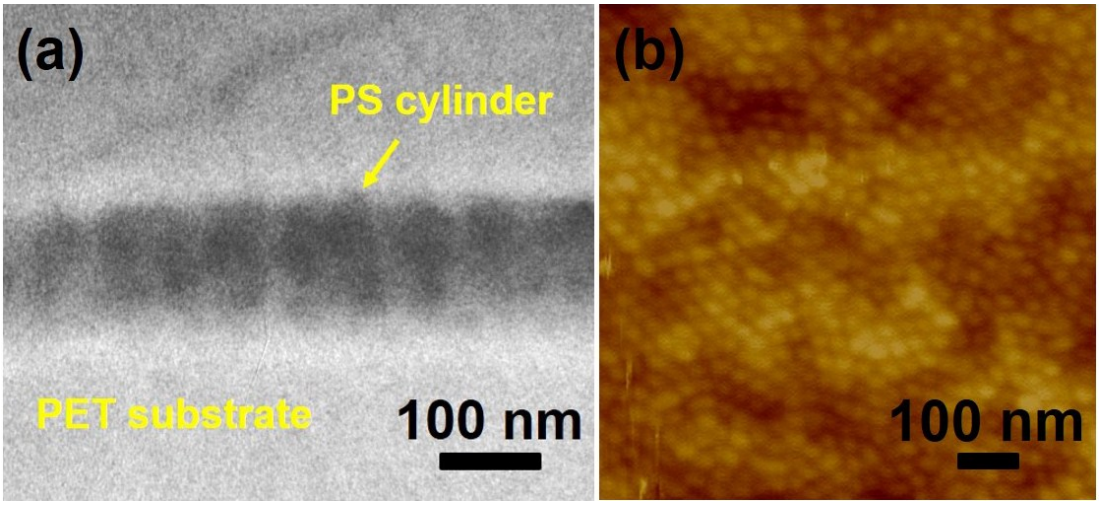

Fig. S14 Cross-sectional TEM (a) and top-view AFM height (b) images of the annealed PS_{100}-*b*-$PMA(Az)_{44}$ film on PET sheet.